Published in final edited form as:
Cell. 2012 February 17; 148(4): 702–715. doi:10.1016/j.cell.2011.12.026.

A sterol binding protein integrates endosomal lipid metabolism with TOR signaling and nitrogen sensing

Carl J. Mousley[1,†], **Peihua Yuan**[1], **Naseem A. Gaur**[2], **Kyle D. Trettin**[1], **Aaron H. Nile**[1], **Stephen J. Deminoff**[3], **Brian J. Dewar**[4], **Max Wolpert**[1], **Jeffrey M. Macdonald**[4], **Paul K. Herman**[3], **Alan G. Hinnebusch**[2], and **Vytas A. Bankaitis**[1,†]

[1]Department of Cell & Developmental Biology, Lineberger Comprehensive Cancer Center, University of North Carolina School of Medicine, Chapel Hill, NC 27599-7090 U.S.A

[2]Laboratory of Gene Regulation and Development, Eugene Shriver National Institute of Child Health and Human Development, National Institutes of Health, 6 Center Drive, Bethesda, MD 20892 U.S.A

[3]Department of Molecular Genetics and Microbiology, The Ohio State University, Columbus, OH 43210 U.S.A

[4]Department of Biomedical Engineering, University of North Carolina School of Medicine, Chapel Hill, NC 27599-7575 U.S.A

SUMMARY

Kes1, and other oxysterol binding protein (OSBP) superfamily members, are involved in membrane and lipid trafficking through trans-Golgi network (TGN) and endosomal systems. We demonstrate that Kes1 represents a sterol-regulated antagonist of TGN/endosomal phosphatidylinositol-4-phosphate signaling. This regulation modulates TOR activation by amino acids, and dampens gene expression driven by Gcn4; the primary transcriptional activator of the general amino acid control regulon. Kes1-mediated repression of Gcn4 transcription factor activity is characterized by nonproductive Gcn4 binding to its target sequences, involves TGN/endosome-derived sphingolipid signaling, and requires activity of the cyclin-dependent kinase 8 (CDK8) module of the enigmatic ‘large Mediator’ complex. These data describe a pathway by which Kes1 integrates lipid metabolism with TORC1 signaling and nitrogen sensing.

Keywords

Kes1; endosomal signaling; TOR signaling; Gcn4; Mediator

[†]co-Corresponding Authors: TEL: 919-962-9870 FAX: 919-966-1856, mousley@email.unc.edu; vytas@med.unc.edu.

Online Supplemental Material. Suppl. Fig. S1 describes properties of Kes1 sterol-binding mutants. Suppl. Fig. S2 describes effects of Kes1 and mutant Kes1 on TGN/endosomal trafficking. Suppl. Fig. S3 documents induction of autophagy by Kes1/kes1^{Y97F} expression and role of autophagy in arrested cell viability. Suppl. Fig. S4 shows metabolomics profiling data. Suppl. Fig. S5 shows Kes1 modulation of TORC1 signaling. Suppl. Fig. S6 documents Kes1/kes1^{Y97F} inhibit activation of the GAAC. Suppl. Fig S7 shows miconazole-evoked super-recruitment of Kes1 to TGN/endosomes inactivates the GAAC, that Kes1 regulates sphingolipid metabolism, and that sphingoid base feeding inactivates the GAAC. Suppl. Tables S1 and S2 list yeast strains and plasmids.

INTRODUCTION

Golgi and endosomes are dynamic organelles that combine physical properties of stable compartments with features consistent with a cycle of self-organized renewal and maturation (Glick and Nakano, 2009). These compartments are key membrane sorting stations and active sites of intracellular signaling. How Golgi/endosomal trafficking and signaling functions are coordinated is not understood, but a lipid signaling interface is an attractive mechanism given the established link between lipid metabolism and membrane trafficking in these compartments. Lipid-exchange proteins play important roles in coordinating lipid metabolism with the actions of protein components of the membrane trafficking machinery in the trans-Golgi network (TGN) and the endosomal membrane system (Bankaitis et al., 2010; Graham and Burd, 2011).

Trafficking through the yeast TGN and endosomal systems is regulated by two lipid-exchange proteins which execute opposing activities (Cleves et al., 1991; Fang et al., 1996). The phosphatidylinositol (PtdIns)/phosphatidylcholine (PtdCho) transfer protein Sec14 is the pro-trafficking member of this pair. Sec14 acts as a coincidence sensor that couples PtdCho metabolism with PtdIns-4-phosphate production (PtdIns-4-P; Schaaf et al., 2008; Bankaitis et al., 2010). PtdIns-4-P is an essential potentiator of membrane trafficking in the TGN/endosomal system (Hama et al., 1999; Rivas et al., 1999; Graham and Burd, 2011). The Sec14 antagonist is Kes1/Osh4 -- one of the 7 yeast members of the oxysterol binding protein (OSBP) superfamily (Fang et al., 1996). Kes1 dampens PtdIns-4-P signaling in TGN/endosomes (Li et al., 2002; Fairn et al., 2007; Stefan et al., 2011). Why cells engineer a Sec14/Kes1 ‘tug-of’war’ into the TGN/endosomal trafficking design remains unclear.

Kes1 is a PtdIns-4-P and sterol-binding protein. PtdIns-4-P binding is a biologically important Kes1 activity and is required for Kes1 homing to TGN/endosomal membranes (Li et al., 2002). With regard to sterol binding, Kes1 is suggested to serve as a diffusible sterol carrier (Im et al., 2005; Schulz et al., 2009). Carrier models are confronted with the rapid rate at which sterol shuttles between membranes via non-vesicular pathways, however (Mesmin and Maxfield, 2009), and measured rates for Kes1-mediated sterol transport in vitro are too slow to account for such rapid flux. New data argue that OSBPs have no role in sterol transport (Georgiev et al., 2011). This controversy underscores our lack of knowledge regarding how Kes1 translates sterol-binding activity to TGN/endosomal trafficking functions, and how Kes1 coordinates its dual PtdIns-4-P and sterol-binding activities.

Herein, we report that Kes1 integrates multiple aspects of lipid metabolism in distal stages of the secretory pathway with TORC1 and nitrogen signaling. Kes1 couples TGN/endosomal sterol and PtdIns-4-P status with sphingolipid (SL) signaling from this endomembrane system. We show that Kes1-regulated SL-signaling in TGN/endosomal membranes attenuates activities of TORC1 and Gcn4, a primary transcription factor for control of amino acid homeostasis. Finally, we report that SL-regulated attenuation of Gcn4 activity requires a functional CDK8 module of the ‘large Mediator’ complex which regulates RNA polymerase II holoenzyme activity. These results introduce new conceptual frameworks for interpreting how Kes1, and other Kes1-like OSBPs, link membrane trafficking and lipid signaling with cell proliferation and transcriptional programs that respond to nitrogen stress.

RESULTS

Kes1 defective in sterol binding retains biological activity

Assignment of Kes1 as a TGN/endosomal trafficking ‘brake’ derives from loss-of-function phenotypes recorded in complex genetic backgrounds (e.g. ‘bypass Sec14’; Cleves et al.,

1991; Fang et al., 1996; Li et al., 2002). The effects of a genuine trafficking brake should also be apparent in otherwise wild-type (WT) genetic backgrounds. Because Kes1 is a nonessential protein in vegetative cells, the function was probed in cells producing excess Kes1. The effects of acute elevations in Kes1 expression were monitored in WT yeast using an inducible system where *KES1* and *kes1* alleles of interest were placed under control of a doxycycline (Dox)-repressible promoter. Three Kes1 derivatives were expressed in parallel: (i) a biologically inactive kes1^{R236E,K242E,K243E} triple mutant (kes1^{3E}) unable to target to TGN/endosomal membranes because it is defective in PtdIns-4-P binding (Li et al., 2002), (ii) the sterol-binding mutant kes1^{Y97F} (Im et al., 2005), and (iii) a second putative sterol-binding mutant (kes1^{T185V}). The $T_{185}V$ substitution, like $Y_{97}F$, is predicted to disrupt the ordered water chain which stabilizes sterol binding within the Kes1 lipid binding pocket (Suppl. Fig. S1A).

Kes1 and its mutant derivatives were further characterized. [^{3}H]-Cholesterol binding to Kes1 and kes1^{3E} was saturable (apparent $K_d \approx 0.5–0.8\mu M$) and specific on the basis of its sensitivity to competition by unlabeled cholesterol (Suppl. Figs. S1B, S1C). In agreement with structural data (Im et al., 2005), the saturation binding data demonstrated both Kes1 and kes1^{3E} bound [^{3}H]-cholesterol in a ca. 1:1 stoichiometry (B_{max}=1.2 pmol sterol bound/ pmol protein). The $Y_{97}F$ and $T_{185}V$ substitutions each diminished specific cholesterol binding to the extent that saturation binding was not attainable. We estimate the binding affinities to be >70X weaker than those measured for Kes1 and kes1^{3E} (Suppl. Fig. S1C). Gel filtration and circular dichroism assays confirmed that kes1^{Y97F} and kes1^{T185V}, like Kes1, were well-folded monomeric proteins (Suppl. Fig. S1D. S1E).

Introduction of P_{DOX}*::KES1*, P_{DOX}*::kes1*^{Y97F}, P_{DOX}*::kes1*^{T185V}, or P_{DOX}*::kes1*^{3E} vectors into yeast did not impair cell growth when the host yeast cells were cultured under non-inducing conditions (in Dox-replete media). Induced Kes1 expression by Dox withdrawal severely inhibited cell growth while kes1^{3E} expression had no such detrimental effect (Fig. 1A). Unexpectedly, expression of the purportedly nonfunctional kes1^{Y97F} and kes1^{T185V} mutants also arrested growth of WT yeast (Fig. 1A). The inducible P_{DOX} expression system elevated protein levels ca. 5-fold (relative to endogenous Kes1) following Dox withdrawal (Fig. 1B) -- indicating the inhibitory effects of kes1^{Y97F} and kes1^{T185V} were not results of excessive expression relative to Kes1 or kes1^{3E}. Toxicity of kes1^{Y97F} and kes1^{T185V} did not require strongly enhanced production. Yields of WT yeast transformants per unit DNA were reduced ca. 100-fold for YCp(*kes1*^{Y97F}) and YCp(*kes1*^{T185V}) plasmids, relative to YCp(*KES1*) and YCp(*kes1*^{3E}). These YCp vectors drive only modest constitutive expression of the Kes1 derivatives (2X relative to endogenous Kes1; Suppl. Fig. S1F). These data indicate kes1^{Y97F} and kes1^{T185V} are more potent inhibitors of cell growth than is Kes1 -- a result incongruent with reports that loss of sterol binding inactivates Kes1 (Im et al., 2005; Schultz et al., 2009). Although OSBPs are reported to function in concert with FFAT receptors (VAPs; Stefan et al., 2011), Kes1-evoked arrest was indifferent to combinatorial ablation of VAP structural genes (*SCS2*, *SCS22*).

Kes1 is unique amongst the yeast OSBPs in its privileged interaction with Sec14-dependent pathways in TGN/endosomal trafficking (Fang et al., 1996). This specificity is reflected in the growth inhibition assay. High-level expression of Hes1 (Osh5; the protein most similar to Kes1), the sterol-binding-defective hes1^{Y97F}, or Osh7 did not compromise cell proliferation.

Lipid-binding and Kes1 association with TGN/endosomes

Two lines of evidence show sterol binding controls Kes1 association with TGN/endosomes. First, whereas Kes1-GFP adopted both diffuse cytosolic and punctate distributions in cells, kes1^{Y97F}-GFP localized predominantly to punctate structures (Fig. 1C). These

compartments were identified as TGN/endosomes because these load with FM4-64 under conditions where the tracer marks endocytic compartments (Fig. 1D). Fractionation analyses also show increased kes1^{Y97F} membrane association (Suppl. Fig. 2A). In addition, Our finding that challenge of cells with a sterol synthesis inhibitor (miconazole) provoked Kes1-GFP super-recruitment to punctate compartments loaded with FM4-64 (Fig. 1E), also suggests sterol binding releases Kes1 from TGN/endosomes..

Enhanced association of Kes1- and kes1^{Y97F} with TGN/endosomes also requires PtdIns-4-P binding activity and robust Pik1-dependent PtdIns-4-P synthesis. Introduction of kes1^{3E} PtdIns-4-P binding defects into the context of kes1^{Y97F} had the effect of: (i) abrogating recruitment of the kes1^{Y97F} sterol-binding-defective mutant to TGN/endosomes (Fig. 1G), and (ii) relieving kes1^{Y97F}-mediated growth arrest (Fig. 1H). Moreover, shift of *pik1-101^{ts}* yeast to 37°C, a condition non-permissive for Pik1-mediated PtdIns-4-P production, released kes1^{Y97F}-GFP from TGN/endosomal membranes (Fig. 1F).

Kes1 restricts PtdIns-4-P availability

Enhanced Kes1 recruitment to TGN/endosomes interfered with localization of the GOLPH3-GFP PtdIns-4-P sensor to this membrane system. In agreement with Wood et al. (2009), GOLPH3-GFP localized to TGN/endosomes in WT cells. This localization is PtdIns-4-P dependent as indicated by release of GOLPH3-GFP upon Pik1 inactivation (Fig. 2A). The GOLPH3-GFP chimera also distributed to TGN/endosomes when WT cells bearing YCp(*P$_{DOX}$::KES1*) or YCp(*P$_{DOX}$::kes1^{Y97F}*) were cultured in non-inducing medium (Fig. 2B). Kes1/kes1^{Y97F} expression released a significant fraction of GOLPH3-GFP from TGN/endosomes (Fig. 2B). Quantitative imaging analyses recorded 3-fold reductions in puncta fluorescence intensity relative to cytosol under those conditions (n=150, p = 0.0009 and p = 0.0003). [^{3}H]-Inositol labeling showed no diminution of bulk PtdIns-4-P, or bulk levels of other phosphoinositides, in the face of Kes1/kes1^{Y97F} expression (Fig. 2C). We conclude Kes1 and kes1^{Y97F} sequester PtdIns-4-P without stimulating its degradation.

Kes1 impairs trafficking

The ability of Kes1 to bind PtdIns-4-P suggests Kes1 interferes with interaction of this phosphoinositide with its pro-secretory effectors. Several independent assays demonstrate that enhanced Kes1 activity impairs TGN/endosomal dynamics. Pulse-radiolabeling experiments show carboxypeptidase Y (CPY) trafficking to the vacuole was inhibited by Kes1, kes1^{Y97F} or kes1^{T185V} (Fig. 2D). Trafficking of the Snc1 v-SNARE and the bulk endocytic tracer FM4-64 were also compromised by Kes1, kes1^{Y97F} or kes1^{T185V} (Fig. 2E). Normally, FM4-64 is internalized from the plasma membrane into endosomal compartments within 7.5 min of chase, and a significant fraction of the cell-associated FM4-64 is detected in the vacuole by that time-point. The non-vacuolar FM4-64 pool chases from endosomes to vacuoles during the remainder of the time-course (Suppl. Fig. S2C). FM4-64 trafficking was interrupted in cells with enhanced Kes1, kes1^{Y97F} or kes1^{T185V} activities; >80% and >40% of cells presented solely punctate endosomal profiles after 15 and 30 min of chase. By 30 min, only 5% of the Kes1-, kes1^{Y97F}- or kes1^{T185V}-expressing cells exhibited vacuolar labeling profiles (Suppl. Fig. S2C).

Trafficking defects were recorded for the general amino acid permease Gap1 (Suppl Fig. S2D), and the defects in uptake of [^{35}S]-amino acids observed for yeast with enhanced Kes1/kes1^{Y97F} activity were also consistent with defects in amino acid permease trafficking to the plasma membrane (Suppl Fig. S2B).

Kes1 induces autophagy

Kes1/kes1^{Y97F}-induced membrane trafficking defects notwithstanding, electron microscopy failed to record the typical accumulation of cargo-engorged TGN/endosomes. Instead, intravacuolar vesicles (diameter ~ 350 nm) were observed in >60% of cells expressing Kes1/kes1^{Y97F} (Fig. 3A). These morphologies report that Kes1/kes1^{Y97F}–arrested cells were engaged in autophagy while bathed in nutrient-sufficient medium. Two other phenotypes support this diagnosis. First, we measured autophagic import from the cytoplasm of a modified alkaline phosphatase zymogen (Pho8Δ60) into the vacuole lumen where Pho8Δ60 is activated (Noda et al., 1995). Pho8 60 activity was elevated 3.8- and 4.2-fold in the face of excess Kes1 and kes1^{Y97F} (Fig. 3B). This enhancement was abrogated by *atg1Δ*, an allele which blocks autophagy at an early stage (Suppl. Fig. S3A). Second, the Atg18 subunit of the pre-autophagosome was recruited to a juxtavacuolar location in Kes1/kes1^{Y97F}-arrested cells in a manner similar to that evoked by NH_4^+-starvation (Suppl. Fig. S3B, S3C).

Kes1/kes1^{Y97F}–mediated growth arrest is not accompanied by loss of viability, even after 20 days, indicating cell quiescence. Survival requires active autophagy, however. Arrested cells rapidly lose viability if incompetent for initiating autophagy (*atg1Δ* mutants), or if vacuolar protease activity is compromised (Suppl. Figs. S3D, S3E). Interestingly, Kes1/kes1^{Y97F}–arrested *atg1Δ* cells accumulated cargo-engorged TGN/endosomes in the cytoplasm, while interference with vacuolar degradative functions resulted in membrane accretion in the vacuole lumen (Suppl. Fig, S3F). These observations indicate the affected compartments are cleared by autophagy in Kes1/kes1^{Y97F}–arrested cells and degraded in the vacuole – explaining our initial failure to observe these structures by electron microscopy.

Kes1 impairs amino acid homeostasis

The autophagy phenotype suggested metabolic imbalances in cells with elevated Kes1 activity. A metabolomic signature for Kes1/kes1^{Y97F}–arrested yeast was established by profiling methanol-soluble small molecules by ^{1}H-NMR (Suppl. Fig. S4A). Unsupervised Principal Component Analysis (PCA) deconvoluted the NMR spectra, and PCA scores plots revealed informative variances in the first principal component (PC1; Fig. 3C). These variances clustered along compact regions of the PC1 axis and accounted for 51% of the total variance in the data set. The second principal component (PC2) further distinguished Kes1- from kes1^{Y97F}-expressing cells. Variances were again confined to narrow windows of the PC2 axis (Fig. 3C). The discriminating methanol-soluble analytes were identified. Shown in Fig. 3D is a comparison of selected metabolites from Kes1/kes1^{Y97F} –arrested cells and mock controls. Pools of 60% of the assignable amino acids were reduced at least 2-fold in the arrested cells. Most prominent were diminutions in Arg, Asn, Asp, Glu, Gln, Thr, and Trp pools (Suppl. Fig. S4B).

Amino acid resuscitation of arrested cells

A concentrated Asn/Glu/Gln/Arg (NEQR) cocktail rescued growth and amino acid pools of Kes1/kes1^{Y97F}-arrested cells (Fig. 3E) – even though these cells are genetically NEQR prototrophs. Yet, the trafficking defects associated with enhanced Kes1/kes1^{Y97F} activity remained unresolved. EM analyses demonstrated that NEQR-rescued cells, unlike Kes1/kes1^{Y97F}-arrested cells, accumulated cargo-engorged TGN/endosomes typically associated with trafficking defects through this system (Suppl. Fig. S4C).

The NEQR data demonstrate Kes1/kes1^{Y97F}-induced arrest derives from amino acid-deficiencies, rather than from trafficking defects per se. The nature of the amino acid-homeostatic problem is the focus of the remainder of this work. Several lines of evidence demonstrate TORC1 activity is inversely proportional to potency of the Kes1 trafficking brake. First, phosphorylation of the TORC1 substrate Atg13 was reduced by Kes1/kes1^{Y97F}

expression (Fig. 3F). This effect was accompanied by phospho-eIF2α accumulation – a hallmark of reduced TORC1 activity (Zaman et al., 2008). Second, genome content assays scored a G_1 block in Kes1/kes1^{Y97F}-arrested cells (Suppl. Fig. S4D). This block exhibits activated Rim15 signatures; a diagnosis of predisposal for entry into G_0. Third, *sec14-1^{ts}* yeast (harbor diminished activity for the pro-trafficking Sec14) were more rapamycin sensitive than isogenic WT strains. Increased rapamycin sensitivity was suppressed by *kes1Δ* (Fig. 3G). Furthermore, rapamycin-treated *kes1Δ* cells accumulated less phospho-eIF2α than did isogenic WT cells (Suppl. Fig. S5A), and both *sec14-1 ^{ts} kes1Δ* and WT *kes1Δ* yeast showed increased rapamycin-resistance relative to WT controls (Figs. 3G, 3H). By contrast, a 2-fold elevation in *KES1* expression rendered a *sec14-1 ^{ts} cki1Δ* 'bypass Sec14' mutant hypersensitive to rapamycin (Suppl. Fig. S5B). In all cases, the relative drug sensitivities reflected magnitude of rapamycin-induced phospho-eIF2α accumulation in these strains (see below).

Amino acids promote TORC1 signaling by potentiating Gtr1 and Gtr2 GTPase activities (Binda et al., 2009), and neither casamino acids nor NEQR revived growth of Kes1/kes1^{Y97F}–arrested *gtr1Δ* or *gtr2Δ* yeast (Suppl. Fig. S5C). NEQR resuscitated growth of Kes1/kes1^{Y97F}-arrested *spo14Δ* and *scs2Δ scs22Δ* mutants. These data demonstrate that neither phospholipase D nor FFAT receptors (VAPs) are required for the NEQR effect, but that Gtr-mediated activation of TORC1 is.

Kes1 and Gcn4-dependent transcriptional regulation

The general amino acid control (GAAC) pathway is a major mechanism for amino acid homeostasis. The GAAC is activated by Gcn2-mediated phosphorylation of eIF2α, a modification that reduces eIF2α activity and promotes translation of the Gcn4 transcription factor ORF (Hinnebusch, 1997). The sensing component of the GAAC is engaged in Kes1/kes1^{Y97F}-arrested yeast as evidenced by phospho-eIF2α accumulation (Fig. 4A; Suppl. Fig. S5D). Yet, downstream induction of the GAAC fails, as measured by induced *HIS4* and *ARG1* transcription (Fig. 4B, Suppl. Fig. S6A). In contrast, Gcn2 induced Gcn4-independent expression of *ARO9* and *ARO10* tryptophanase genes (Chen et al., 2009; Staschke et al., 2010) ca. 7-fold in Kes1/kes1^{Y97F}-arrested cells (Suppl. Fig. S6B). This induction likely contributed to the 50-fold reductions in Trp pools in those cells.

To assess Gcn4 status under conditions of enhanced Kes1 activity, we employed a sensitized system where *sec14-1^{ts} cki1Δ* cells arrest in response to 2-fold elevations in Kes1 level (Fang et al., 1996). Kes1-dependent increases in phospho-eIF2α were reproduced in that genetic background (Suppl. Fig. S6C). However, translational derepression of *GCN4* was severely diminished (Suppl. Fig. S6D). The consequences are growth defects in minimal media supplemented with the His analog 3-aminotriazole (3-AT; Suppl. Fig. S6E). Consistent data were also obtained from otherwise WT cells subjected to Kes1/kes1^{Y97F}-growth arrest. Reduced Gcn4 accumulation was observed in those cells under conditions where Gcn4 production is normally induced by 3-AT (Fig. 4C). Yet, bypass of Gcn4 translational control (Gcn4^{c}) failed to activate the GAAC in Kes1/kes1^{Y97F} arrested cells (Fig. 4D; Suppl. Fig. S6F) -- despite sustained Gcn4^{c} protein levels (Suppl. Fig. S5F). NEQR administration revived the GAAC in those cells (Fig. 4E, Suppl. Fig. S6G).

Inactivation of the GAAC without increased Kes1 expression

The data predicted that physiological levels of Kes1 expression would silence the GAAC upon: (i) enhanced Kes1 recruitment to TGN/endosomes, or (ii) imposition of TGN/endosomal trafficking defects by reducing activities of pro-exocytic factors. Kes1 load on TGN/endosomes was increased by challenging yeast with sub-growth inhibitory levels of

the sterol synthesis inhibitor miconazole. The intoxicated cells failed to respond appropriately to 3-AT challenge (Suppl. Fig. S7A).

The effects of Kes1/kes1^{Y97F} expression on GAAC activity were recapitulated in a mutant that expresses normal levels of Kes1, but is compromised for two factors that promote TGN/endosomal trafficking (*sec14-1^{ts} tlg2*Δ; Fig. 4F). The quiescent GAAC was not only revived by *kes1*Δ, but was constitutively induced in *sec14-1^{ts} tlg2*Δ *kes1*Δ mutants (Fig. 4F). This effect was not a general effect of 'bypass Sec14' mutations as *cki1*Δ failed to re-activate the GAAC in *sec14-1^{ts} tlg2*Δ yeast.

Kes1 and SL metabolism

The GAAC defects observed in *sec14-1^{ts} tlg2*Δ cells were accompanied by elevated ceramide, sphingoid base, and sphingoid base-phosphate mass (Suppl. Fig. S7B). Kes1/kes1^{Y97F}–arrested yeast similarly exhibited increases in dihydro- and phytoceramide mass (DHC, PHC), and dihydro- and phytosphingosine (DHS, PHS) mass (Fig. 5A). Increases were also measured for the sphingoid base-phosphates (Fig. 5A). Incorporation of *kes1Δ* into the *sec14-1^{ts} tlg2*Δ double mutant normalized intracellular ceramide, sphingoid base, and sphingoid base-phosphate mass (Suppl. Fig. S7B). These lipidomics data suggested that SL metabolism links TGN/endosome trafficking status to nuclear transcriptional outcomes.

Sphingosine feeding compromises the GAAC

If Kes1 extinguishes the GAAC via a SL-signaling mechanism, alterations in SL mass by means that do not affect cellular Kes1 levels should also silence the GAAC. WT yeast were challenged with sub-growth inhibitory levels of PHS. Histidine stress was superimposed on this condition by 3-AT challenge. While cell proliferation was unaffected by individual PHS or 3-AT challenge, both growth-inhibition and blunting of the GAAC transcriptional response was elicited by dual challenge (Fig. 5B; Fig. 5C; Suppl. Fig. S7C). The PHS-mediated inhibition of cell growth was apparent in the face of constitutive expression of Gcn4 (Fig. 5D), and *HIS4* and *ARG1* transcription was strongly diminished under that condition as well (Fig. 5E; Suppl. Fig. S7D). TGN/endosomal trafficking was unperturbed under these conditions.

Sensitivity of the GAAC to PHS challenge requires Kes1 as *kes1Δ* cells exhibited enhanced resistance to PHS (Fig. 5B). Gcn4-dependent *HIS4* and *ARG1* transcription was similarly resistant to dual PHS and 3-AT challenge in *kes1Δ* cells (Fig. 5C; Suppl. Fig. S7C). Finally, ectopic expression of the yeast Ypc1 phytoceramidase revived the GAAC in the face of Kes1- and PHS-challenge (Suppl. Figs. S7E, S7F). These data connect SL metabolism with GAAC activity, and implicate ceramide as a key regulatory lipid.

Nonproductive binding of enhancer elements by Gcn4

Chromatin immunoprecipitation experiments interrogated Gcn4 status on the *ARG1* promoter in vivo. Gcn4 binding at the *ARG1* UAS was induced by 3-AT in both mock-treated yeast and in yeast challenged with 15 μM PHS (Fig. 6A). Enhanced RNA Polymerase II (Rpb3) occupancy evoked by 3-AT was dampened by PHS at the promoter and at 5′ and 3′ locations in *ARG1* coding sequences (Fig. 6B). These results report only modest defects in the ability of UAS-bound Gcn4 to stimulate assembly of the pre-initiation complex (PIC) at the *ARG1* promoter. Additional levels of regulation must be engaged downstream of PIC assembly to account for the potent block of induced *ARG1* transcription by PHS.

Large Mediator and GAAC repression

Core Mediator is recruited to promoters by Gcn4, and plays a key role in stimulating PIC assembly (Govind et al., 2005). The CDK8 module of the large Srb-Mediator complex, is implicated in transcriptional repression and in transcriptional checkpoints (Myers and Kornberg, 2000; Hengartner et al., 1998; Taatjes, 2010). We find Gcn4-inactivation in both Kes1- and PHS-intoxicated yeast required a functional Srb10; the cyclin dependent kinase subunit of the CDK8 module -- *srb10Δ* yeast were resistant to Kes1/kes1^{Y97F} -arrest, or combinatorial PHS/3-AT challenge (Fig. 6C,D). These phenotypes coincided with rejuvenated Gcn4-dependent *HIS4* and *ARG1* transcription (Fig. 6E). The same results were obtained upon deletion of the structural genes encoding the other three components of the CDK8 module (Srb8,9,11). Thus, the CDK8 module compromises ability of Mediator to stimulate GAAC activation in response to altered TGN/endosomal SL signaling.

Discussion

Herein, we demonstrate Kes1 uses its sterol- and PtdIns-4-P-binding activities to integrate multiple pathways of endosomal lipid metabolism with the activity of TORC1-dependent proliferative pathways and transcriptional control of nitrogen signaling. This Kes1-regulated pathway provides mechanistic insights as to why GAAC activation by Gcn4 is sensitive to trafficking defects involving endosomal compartments (Mousley et al., 2008; Zhang et al., 2008). Finally, these findings generate conceptual frameworks for interpreting how Kes1, and other Kes1-like OSBPs, are integrated into eukaryotic cell physiology.

Kes1 Lipid Binding

The data identify Kes1 as a TGN/endosomal ‘trafficking brake’ whose activity depends on PtdIns-4-P binding. The ‘brake’ is attenuated by sterol binding which promotes Kes1 disengagement from PtdIns-4-P in TGN/endosomal membranes. We describe Kes1 as a sterol-regulated rheostat of TGN/endosomal PtdIns-4-P signaling. The interplay between sterol- and PtdIns-4-P binding regulates potency of Kes1-mediated inhibition of PtdIns-4-P-dependent trafficking through this endomembrane system. We cannot reconcile these results with conclusions that sterol-binding defects inactivate Kes1 (Im et al., 2005). Our data indicate Kes1 couples TGN/endosomal sterol status with efficacy of PtdIns-4-P signaling as a sterol sensor. Signaling circuits built on ‘tuning’ principles do not require Kes1 to display the large capacities for sterol exchange demanded by non-vesicular sterol transfer models.

Kes1 and Nitrogen Signaling

A potent Kes1 TGN/endosomal membrane trafficking brake induces G_1/G_0 growth arrest associated with diminished TORC1 activity, induction of autophagy, and depleted amino acid pools. That amino acid homeostatic defects cause growth arrest as demonstrated by the Gtr GTPase-dependence of NEQR-mediated resuscitation of cell proliferation, TORC1 activity and proper amino acid homeostasis in cells with enhanced Kes1 activity. We write a chain of events where Kes1-evoked NH_4^+ starvation compromises TORC1 by attenuating amino acid stimulation of Gtr GTPases.

Asn is a critical component of the NEQR cocktail. We interpret Asn essentiality reports NH_4^+ starvation as a key insult to Kes1-arrested cells because NEQR failed to rescue Kes1-arrest in *asp1Δ* yeast. The Asp1 asparaginase produces Gln by transferring NH_2 from Asn to Glu. Gln is a key reservoir of biosynthetic NH_4^+ (Wise and Thompson, 2010). Yet, Gln supplementation failed to rescue Kes1-mediated growth arrest; suggesting metabolic channeling of Asn is crucial. This concept might be of broad relevance as the Gcn2-Atf4 pathway (Atf4 is mammalian Gcn4) supports Asn-dependent tumor survival (Ye et al., 2010).

Endosomal Signaling and Nuclear Outputs

Resuscitation of Kes1-arrested cells by NEQR occured in the face of unresolved TGN/endosomal trafficking defects -- signifying that the trafficking defects are, by themselves, insufficient to compromise cell proliferation. Growth arrest was driven by a TGN/endosomal SL-derived signal which dampens TORC1 and Gcn4 activities, and leads to an insurmountable nitrogen deficit. The trafficking defects initiated the chain of events in two respects. First, these provided the initial insult to cellular nitrogen status. Amino acid and NH_4^+permeases were not efficiently delivered to the plasma membrane under such conditions – thereby compromising nitrogen acquisition. Second, Kes1/kes1^{Y97F} -mediated trafficking defects increased SL-signal potency with downstream consequences – e.g. transcriptional down-regulation of Gap1 (3X) and of the major NH_4^+-permease Mep2 (8.5X).

Activation of autophagy, and proximal stages of the GAAC, indicated Kes1-arrested yeast register nitrogen stress. Yet, the cells failed to execute a productive GAAC because *GCN4* mRNA translation was blunted. The translational defect might result from Gln deficiency. Gln is an indicator of nitrogen availability, and nitrogen starvation blocks translation of *GCN4* mRNA by induced by phospho-eIF2α (Grundmann et al., 2001). Kes1 signaling also inhibited Gcn4 activity as transcription factor, recapitulating a phenotype we observed in *vps* mutants (Zhang et al., 2008). Hence, the transcriptional defects in *vps* mutants might also involve Kes1 signaling.

What SL biochemistry underlies the mechanism through which endosomal events influence nuclear Gcn4 activities? While the nature of the signal remains to be established, an SL-driven signaling pathway must negotiate the physical separation of these compartments. A diffusible enzyme (SL-activated kinase or phosphatase) might be activated on the endosomal surface and modify nuclear substrates that regulate Gcn4 activity. While the identities of nuclear effectors is unknown, the CDK module of large Mediator is an attractive candidate given functional silencing of Gcn4 requires Srb10. Whether SLs stimulate Srb10 CDK activity is a key question. Gcn4 might represent the effector as we observe an endosome-associated Gcn4 pool (NAG and AGH, unpublished). Epigenetic effects are also plausible as histone deacetylases are inhibited by sphingosine-1-P (Nitai et al., 2009).

Kes1 and homeostatic control

Why engineer a Sec14/Kes1 antagonism into the TGN/endosomal trafficking design? We propose the Sec14/Kes1 ‘tug-of-war’ sets the SL signaling output of a PtdIns-4-P/sterol-regulated endosomal compartment (Fig. 7A). Appropriate tuning of signaling output is crucial because the organelle couples membrane trafficking to local lipid metabolism and, subsequently, to global responses. The Kes1 ‘brake’ on PtdIns-4-P signaling enhances production of bioactive SLs in an endosomal compartment monitored by homeostatic control systems (Fig. 7B). Whereas such a design could be used in physiological contexts (see below), enhanced endosomal SL signaling exerts significant consequences for cell physiology – as manifested by the effects we document on TORC1 and GAAC signaling.

While we focus on the GAAC, the nitrogen control response (NCR) is also silenced in Kes1-arrested cells. The NCR controls nitrogen acquisition via GATA transcription factor-regulated expression of amino acid- and NH_4^+-permeases (e.g. *GAP1*, *MEP2*; Zaman et al., 2008). NEQR supplementation, or Srb10 inactivation, also revive the NCR. NCR defects suggest a mechanism for transcriptional downregulation of *GAP1* and *MEP2* in Kes1-arrested cells.

Broader Implications for OSBPs?

Kes1-like proteins might be physiological modulators of cell proliferation programs. Loss of such activities will be scored under conditions where a trafficking brake needs to be imposed. In that regard, functional ablation of Kes1 compromises cell viability under starvation conditions -- suggesting loss of Kes1 activity hinders cells from adjusting endosomal lipid signaling in response to nitrogen deprivation. The cardinal properties of Kes1-arrested yeast, like those of Sec14-deficient cells, conform to those of post-mitotic cells. Perhaps privileged PtdIns transfer protein::OSBP pairs co-evolved for fine-tuning systems that couple endosomal lipid signaling with cell proliferation. Such modalities could guide cell entry into post-mitotic states, or maintain post-mitotic cell physiology. This concept raises possibilities for OSBPs flexibly coupling membrane trafficking flux and organelle maturation to the fine-tuning of transcriptional programs for organogenesis of tissues populated with post-mitotic cells.

EXPERIMENTAL PROCEDURES

Yeast strains and media

Yeast strain genotypes and plasmids are listed in Suppl. Table S1 and S2. Yeast complex and synthetic complete media and yeast transformation methods were as described (Cleves et al., 1991; Schaaf et al., 2008). Fine chemicals were purchased from Sigma Chemical (St. Louis, MO) and restriction enzymes were from New England Biolabs, Inc. (Ipswich, MA). YCp(P_{DOX}*::KES1*) transformants, and mutant derivatives thereof, were maintained in the presence of 10μg/ml Dox. To induce expression, cells were washed 4X in ddH_2O and resuspended in fresh Dox-free media for a minimum of 8 hours. Amino acids (Asn, Glu, Gln, and Arg) were added at a final concentration of 0.2% (w/v). YCp(P_{CUP1}-$ATG13^{HA}$) expression was induced by the addition of 100μM $CuSO_4$ for 1 hour.

Expression vectors

To generate YCp(P_{DOX}*::KES1*), the *KES1* ORF was PCR amplified with oligonucleotides clamped with *PmeI* and *PstI* restriction sites at the 5′ and 3′ ends. The 1319 bp fragment was subcloned into pCM189 (Gari et al., 1997). Primer sequences are available from the authors by request.

Sterol binding

The sterol:detergent micelle assay of Infante et al. (2007) was used to measure sterol binding with minor modification. Details are in Supplementary Materials.

Fluorescence microscopy

Cells grown at 30°C were incubated with a final concentration of 10μM FM4-64 (Molecular Probes) for 10 min. Labeling was stopped with 10mM NaN_3/NaF. For GFP-Snc1 imaging, cells were cultured at 30°C. Images were collected with a Nikon E600 microscope equipped with a Princeton Instruments 512 × 512 back-illuminated frame-transfer CCD camera. Metamorph (Universal Imaging Corp.) was used to capture images.

Transmission electron microscopy

Yeast were grown to mid-logarithmic phase (OD_{600nm} = 0.3). Ten OD_{600nm} units of cells were isolated, and fixed in 3% glutaraldehyde. Cells were converted to spheroplasts with zymolyase, stained with 2% osmium tetroxide and 2% uranyl acetate, dehydrated in a 50, 70, 90% ethanol series, and washed in 100% ethanol and 100% acetone, respectively. Cells were embedded in Spurr's resin, sections prepared as described (Adamo *et al*., 1999), and

visualized at 80kV on a FEI Tecnai 12 electron microscope. Images were captured using Gatan micrograph 3.9.3 software.

Metabolic labeling and immunoprecipitation

Yeast were grown in minimal media lacking methionine and cysteine to mid logarithmic phase (OD_{600nm} = 0.5) and radiolabeled with [^{35}S]-amino acids (Translabel; New England Nuclear; 100 μCi/ml). Chase was initiated by introduction of unlabeled methionine and cysteine (2 mM each, final concentration) for the specified time, and chase was terminated by addition of trichloroacetic acid (5% w/v -- final concentration). Immunoprecipitation of CPY with rabbit antiserum and resolution by SDS-PAGE and autoradiography were performed as previously described (Cleves et al., 1991; Schaaf et al., 2008).

Determination of LacZ activity and RT-PCR

Yeast strains were transformed with plasmid p180 (Hinnebusch, 1985) and LacZ activity assayed (Mousley et al., 2008). For RT-PCR assays, total RNA was isolated from cells and 1μg was used to template reverse transcription to generate cDNA (20μl final volume). To analyze *HIS4*, *ARG1* or *ACT1* expression, PCR was performed using 1μl of cDNA fraction as template and specific oligonucleotides as primers. Products were quantified with ImageQuant (GE Healthcare Life Science).

Autophagy Assays

Alkaline phosphatase assays that monitor delivery of a cytosolic Pho8 phosphatase reporter to the vacuole lumen by autophagy, and its subsequent proteolytic activation in the vacuole, were performed as described (Stephan et al., 2009).

Sphingolipidomics

Ceramides and sphingoid bases were measured at the Lipidomics Shared Resource facility at the Medical University of South Carolina using normal phase high perfomance liquid chromatography coupled to atmospheric pressure chemical mass spectrometry (Bielawski et al., 2006). Neutral lipids were isolated from yeast extracts generated by pooling three independent cultures of each yeast strain that had been grown at 30°C. ESI/MS/MS analysis of ceramides and internal standards were performed on a Thermo Finnigan TSQ 7000 triple quadruple mass spectrometer operating in a multiple reaction monitoring positive ionization mode. Calibration curves for quantification were constructed by plotting peak area ratios of synthetic standards. Ceramides were normalized to total organic phosphate.

NMR spectroscopy and analysis

Small metabolites were extracted in 50% methanol and reconstituted in 0.5 mM trimethylsilyl-2,2′,3,3′-tetradeuteropropioninc acid in D_2O. ^{1}H NMR spectra were acquired at 16.4T with a Varian INOVA (700 MHz ^{1}H, Varian Instruments) equipped with 5mm indirect cold probe and processed with ACD/1D NMR Manager (version 12.0; Advanced Chemistry Development, Inc., Toronto, ON, Canada). Spectra were phase and baseline corrected, referenced to the TSP peak to 0.00 ppm, and grouped spectra were data-reduced to 250 bins using intelligent bucketing. Principal Component Analysis used SIMCA-P (version 11.0; Umetrics, Umea, Sweden) and Pareto scaling. Individual metabolites were quantified using Chenomx NMR Suite (version 5.1; Chenomx Inc., Edmonton, Canada), with TSP as reference (Dewar et al., 2010). Details are described in Supplementary Materials.

Supplementary Material

Refer to Web version on PubMed Central for supplementary material.

Acknowledgments

This paper is dedicated to the memories of Christian Raetz and Eugene Kennedy. The work was supported by NIH grant GM44530 to VAB. NG and AGH were supported by the Intramural Research Program of the NIH, SJD and PKH NIH grant GM65227 awarded to PKH, and BJD and JMM NIEHS T32EX007126 and GM075941. KDT acknowledges support from the UNC William W. and Ida W. Taylor Honors Mentored Research Fellows Program. We thank Doug Cyr, Scott Moye Rowley, Chris Burd, and Dan Klionsky for strains and plasmids, Colin Stirling for CPY antibody, Chris Stefan, Scott Emr and Maria Cardenas for discussions, and Lora Yanagisawa, Victoria Hewitt and Robert Sons for comments on the manuscript. We acknowledge the UNC Lineberger Comprehensive Cancer Center Genome Analysis and Nucleic Acids Core facilities. The authors declare no financial conflicts.

LITERATURE CITED

Bielawski J, Szulc ZM, Hannun YA, Bielawska A. Simultaneous quantitative analysis of bioactive SLs by high-performance liquid chromatography-tandem mass spectrometry. Methods. 2006; 39:82–91. [PubMed: 16828308]

Binda M, Péli-Gulli MP, Bonfils G, Panchaud N, Urban J, Sturgill TW, Loewith R, De Virgilio C. The Vam6 GEF controls TORC1 by activating the EGO complex. Mol Cell. 2009; 35:563–73. [PubMed: 19748353]

Chen H, Huang H, Li X, Tong S, Niu L, Teng M. Crystallization and preliminary X-ray diffraction analysis of ARO9, an aromatic aminotransferase from Saccharomyces cerevisiae. Protein Pept Lett. 2009; 16:450–3. [PubMed: 19356146]

Cleves AE, McGee TP, Whitters EA, Champion KM, Aitken JR, Dowhan W, Goebl M, Bankaitis VA. Mutations in the CDP-choline pathway for phospholipid biosynthesis bypass the requirement for an essential phospholipid transfer protein. Cell. 1991; 64:789–800. [PubMed: 1997207]

Dewar BJ, Keshari K, Jeffries RE, Dzeja P, Graves LM, Macdonald JM. Metabolic assessment of a novel chronic myelogenous leukemia cell line and an imatinib resistant submine by 1H NMR spectroscopy. Metabolomics. 2010; 6:439–450. [PubMed: 20676217]

Fairn GD, Curwin AJ, Stefan CJ, McMaster CR. The oxysterol binding protein Kes1p regulates Golgi apparatus phosphatidylinositol-4-phosphate function. Proc Natl Acad Sci. 2007; 104:15352–15357. [PubMed: 17881569]

Fang M, Kearns BG, Gedvilaite A, Kagiwada S, Kearns M, Fung MKY, Bankaitis VA. Kes1p shares homology with human oxysterol binding protein and participates in a novel regulatory pathway for yeast Golgi-derived transport vesicle biogenesis. EMBO J. 1996; 15:6447–6459. [PubMed: 8978672]

Garí E, Piedrafita L, Aldea M, Herrero E. A set of vectors with a tetracycline-regulatable promoter system for modulated gene expression in Saccharomyces cerevisiae. Yeast. 1997; 13:837–848. [PubMed: 9234672]

Georgiev AG, Sullivan DP, Kersting MC, Dittman JS, Beh CT, Menon AK. Osh Proteins regulate membrane sterol organization but are not required for sterol movement between the ER and PM. Traffic. 2011 [Epub ahead of print]. 10.1111/j.1600-0854.2011.01234.x

Glick BS, Nakano A. Membrane traffic within the Golgi apparatus. Annu Rev Cell Dev Biol. 2009; 25:113–132. [PubMed: 19575639]

Govind CK, Yoon S, Qiu H, Govind S, Hinnebusch AG. Simultaneous recruitment of coactivators by Gcn4p stimulates multiple steps of transcription in vivo. Mol Cell Biol. 2005; 25:5626–5638. [PubMed: 15964818]

Graham TR, Burd CG. Coordination of Golgi functions by phosphatidylinositol 4-kinases. Trends Cell Biol. 2011; 21:113–121. [PubMed: 21282087]

Grundmann O, Mösch HU, Braus GH. Repression of GCN4 mRNA translation by nitrogen starvation in Saccharomyces cerevisiae. J Biol Chem. 2001; 276:25661–71. [PubMed: 11356835]

Hama H, Schnieders EA, Thorner J, Takemoto JY, DeWald D. Direct involvement of phosphatidylinositol-4-phosphate in secretion in the yeast Saccharomyces cerevisiae. J Biol Chem. 1999; 274:34294–34301. [PubMed: 10567405]

Hengartner CJ, Myer VE, Liao SM, Wilspon CJ, Koh SS, Young RA. Temporal regulation of RNA polymerase II by Srb10 and Kin28 cyclin-dependent kinases. Molecular Cell. 1998; 2:43–53. [PubMed: 9702190]

Hinnebusch AG. A hierarchy of trans-acting factors modulates translation of an activator of amino acid biosynthetic genes in Saccharomyces cerevisiae. Mol Cell Biol. 1985; 5:2349–2360. [PubMed: 3915540]

Hinnebush AG. Translational regulation of yeast Gcn4. A window on factors that control initiator t-RNA binding to the ribosome. J Biol Chem. 1997; 272:21661–21664. [PubMed: 9268289]

Im YJ, Raychaudhuri S, Prinz WA, Hurley JH. Structural mechanism for sterol sensing and transport by OSBP-related proteins. Nature. 2005; 437:154–158. [PubMed: 16136145]

Lewis MJ, Nichols BJ, Prescianotto-Baschong C, Riezman H, Pelham HR. Specific retrieval of the exocytic SNARE Snc1p from early yeast endosomes. Mol Biol Cell. 2000; 11:23–38. [PubMed: 10637288]

Li XMP, Rivas M, Fang J, Marchena B, Mehotra A, Chaudhary L, Feng GD, Prestwich, Bankaitis VA. Analysis of oxysterol binding protein homologue Kes1p function in regulation of Sec14p-dependent protein transport from the yeast Golgi complex. J Cell Biol. 2002; 157:63–77. [PubMed: 11916983]

Mesmin B, Maxfield FR. Intracellular sterol dynamics. Biochim Biophys Acta. 2009; 1791:636–645. [PubMed: 19286471]

Mousley CJ, Tyeryar K, Ile KE, Schaaf G, Brost RL, Boone C, Guan X, Wenk MR, Bankaitis VA. Trans-Golgi network and endosome dynamics connect ceramide homeostasis with regulation of the unfolded protein response and TOR signaling in yeast. Mol Biol Cell. 2008; 19:4785–4803. [PubMed: 18753406]

Mueller PP, Hinnebusch AG. Multiple upstream AUG codons mediate translational control of GCN4. Cell. 1986; 45:201–207. [PubMed: 3516411]

Myers LC, Kornberg RD. Mediator of transcriptional regulation. Annu Rev Biochem. 2000; 69:729–749. [PubMed: 10966474]

Nitai C, et al. Regulation of histone acetylation in the nucleus by sphingosine-1-phosphate. Science. 2009; 325:1254–1257. [PubMed: 19729656]

Noda T, Matsuura A, Wada Y, Ohsumi Y. Novel system for monitoring autophagy in the yeast Saccharomyces cerevisiae. Biochem Biophys Res Commun. 1995; 210:126–132. [PubMed: 7741731]

Rivas MP, Kearns BG, Xie Z, Guo S, Sekar MC, Hosaka K, Kagiwada S, York JD, Bankaitis VA. Relationship between altered phospholipid metabolism, diacylglycerol, ‘bypass Sec14’, and the inositol auxotrophy of yeast sac1 mutants. Mol Biol Cell. 1999; 10:2235–2250. [PubMed: 10397762]

Schaaf G, Ortlund E, Tyeryar K, Mousley C, Ile K, Woolls M, Garrett T, Raetz CRH, Redinbo M, Bankaitis VA. The functional anatomy of PL binding and regulation of PIP homeostasis by proteins of the Sec14-superfamily. Molecular Cell. 2008; 29:191–206. [PubMed: 18243114]

Schulz TA, Prinz WA. Sterol transport in yeast and the oxysterol binding protein homologue (OSH) family. Biochim Biophys Acta. 2009; 1771:769–780. [PubMed: 17434796]

Staschke KA, Dey S, Zaborske JM, Palam LR, McClintick JN, Pan T, Edenberg HJ, Wek RC. Integration of general amino acid control and target of rapamycin (TOR) regulatory pathways in nitrogen assimilation in yeast. J Biol Chem. 2010; 285:16893–911. [PubMed: 20233714]

Stefan CJ, Manford AG, Baird D, Yamada-Hanff J, Mao Y, Emr SD. Osh proteins regulate phosphoinositide metabolism at ER-plasma membrane contact sites. Cell. 2011; 144:389–401. [PubMed: 21295699]

Taatjes DJ. The human Mediator complex: a versatile, genome-wide regulator of transcription. Trends in Biochem Sci. 2010; 35:315–322. [PubMed: 20299225]

Wise DR, Thompson CB. Gutamine addiction: a new therapeutic target in cancer. Trends Biochem Sci. 2010; 35:427–433. [PubMed: 20570523]

Ye J, Kumanova M, Hart LS, Sloane K, Zhang H, De Panis DN, Bobrovnikova-Marjon E, Diehl JA, Ron D, Koumenis C. The GCN2-ATF4 pathway is critical for tumour cell survival and proliferation in response to nutrient deprivation. EMBO J. 2010; 29:2082–2096. [PubMed: 20473272]

Zaman S, Lippman SI, Zhao X, Broach JR. How Saccharomyces responds to nutrients. Annu Rev Genet. 2008; 42:27–81. [PubMed: 18303986]

Zhang F, Gaur NA, Hasek J, Kim SJ, Qiu H, Swanson MJ, Hinnebusch AG. Disrupting vesicular trafficking at the endosome attenuates transcriptional activation by Gcn4. Mol Cell Biol. 2008; 28:6796–6818. [PubMed: 18794364]

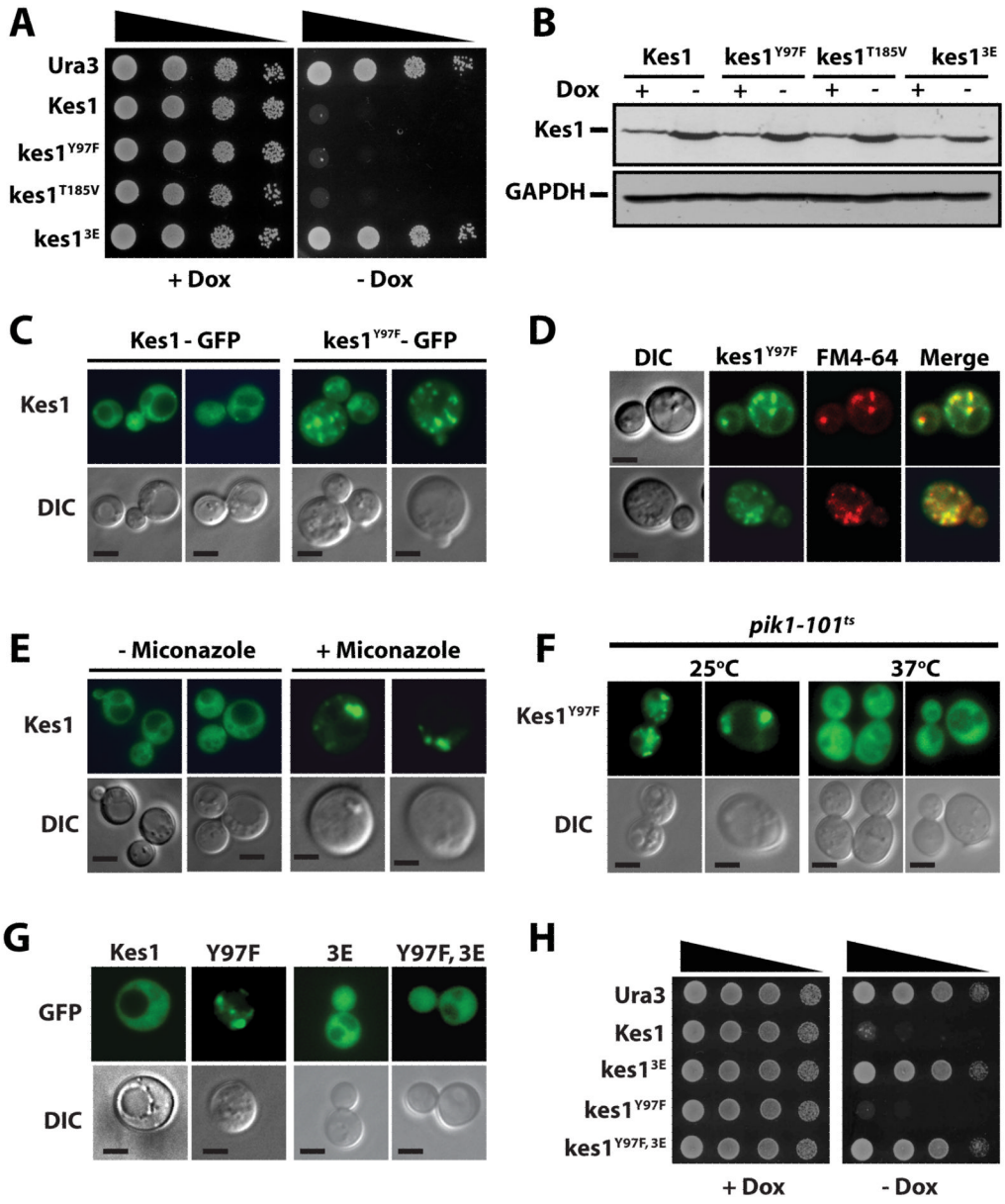

Figure 1.

Sterol binding regulates Kes1 activity. **(A)** WT yeast (CTY182) engineered for Dox-repressible expression of the indicated Kes1 derivatives were spotted in 10-fold dilutions series on uracil-free media +/− Dox (10μg/ml) and incubated at 30°C. **(B)** Lysates were prepared from the strains in (A), normalized for total protein (10μg loaded), and Kes1 and GAPDH were visualized by immunoblotting. **(C)** WT yeast expressing Kes1-GFP or kes1^{Y97F}-GFP were cultured to mid-logarithmic growth phase in uracil-free medium at 30°C. GFP profiles are shown. **(D)** WT yeast expressing kes1^{Y97F}-GFP were pulse-labeled with FM4-64 (10μM) for 10 min and poisoned with a 10 mM NaN_3/NaF cocktail. FM4-64, GFP and merge profiles are shown with corresponding DIC image (bar = 5μm). **(E)** WT yeast expressing Kes1-GFP were challenged with miconazole for 4hrs. GFP profiles are shown. **(F)** *pik1-101^{ts}* cells expressing kes1^{Y97F}-GFP were cultured at 25°C, split and one culture maintained at 25°C while the partner was shifted to 37°C for 1hr prior to imaging. **(G)** Profiles of GFP-tagged versions of indicated Kes1 derivatives are shown with

corresponding DIC images (bar = 5μm). **(H)** WT yeast engineered for Dox-repressible expression of indicated Kes1 derivatives (or mock Ura3 control) were spotted in 10-fold dilutions series on selective media with Dox (10μg/ml) as variable. Also see Suppl. Figs. S1 and S2.

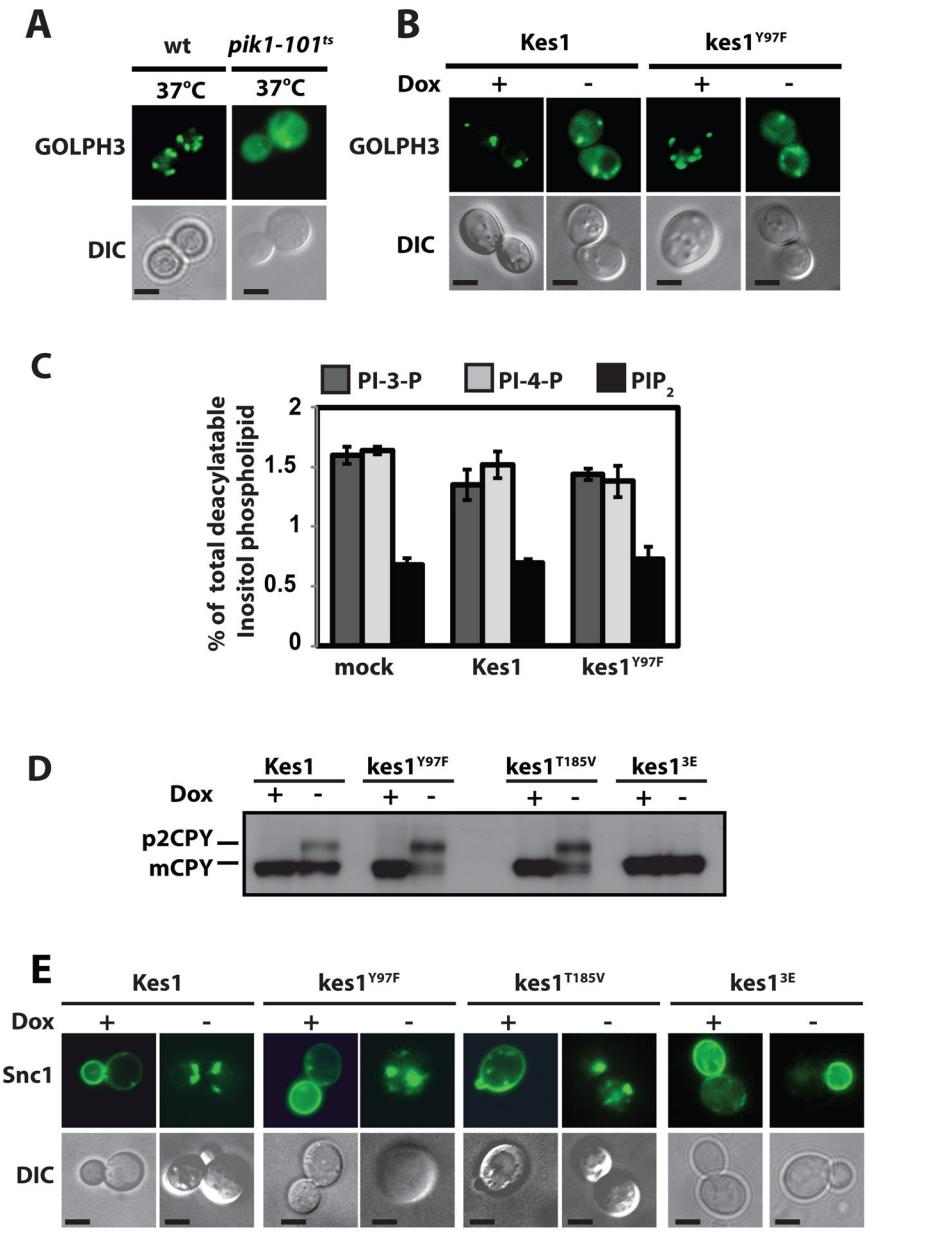

Figure 2.

Kes1 and PtdIns-4-P homeostasis. **(A)** WT and *pik1-101*^{ts} cells expressing GOLPH3-GFP were cultured in uracil-free medium at 25°C and shifted to 37°C for 60 min prior to imaging. Corresponding DIC images are shown at bottom (bar = 5μm). **(B)** WT yeast (CTY8-11Cα) expressing GOLPH3-GFP and indicated Kes1 derivatives were incubated +/− Dox (10μg/ml) for 18 hours. GOLPH3-GFP (top panel) and DIC images (bottom panel) profiles are shown (bar = 5μm). **(C)** WT yeast (CTY182) engineered for Dox-repressible expression of Kes1 derivatives were radiolabeled to steady-state at 30°C with 20 μCi/ml [^{3}H]-Ins +/− Dox as indicated. Fractional incorporation of [^{3}H]-Ins into the deacylated PtdIns-3-P, PtdIns-4-P, and PtdIns(4,5)P_2 species is indicated (n = 4). Error bars represent standard deviation. **(D)** WT yeast (CTY182) expressing the Kes1 derivatives were cultured +/− Dox. Cells were pulse-radiolabeled with [^{35}S]-amino acids (15 min). After 30 min of chase, immunoprecipitated CPY species were analyzed by SDS-PAGE and autoradiography.

p2 CPY and mCPY are indicated. **(E)** WT yeast (CTY182) expressing Kes1 species (−Dox) and corresponding non-expressing controls (+Dox), were examined for GFP-Snc1 distribution. DIC images are shown at bottom (bar = 5μm). Also see Suppl. Fig. S2.

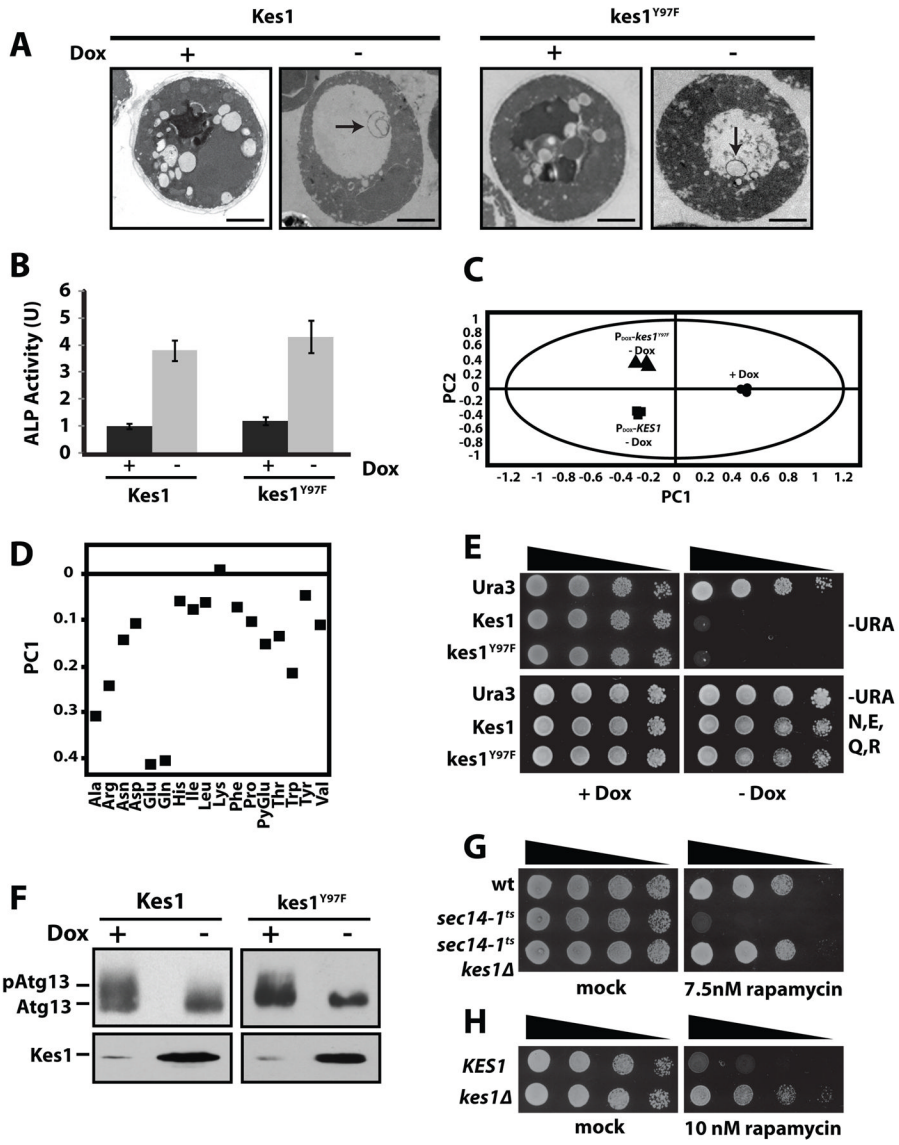

Figure 3.

Kes1 and amino acid homeostasis. **(A)** WT yeast cells (CTY182) producing Kes1 derivatives (−Dox) and corresponding non-expressing controls (+Dox; 10μg/ml) were analyzed by EM. Representative images are shown (bar = 1μm). Intra-vacuolar vesicular profiles (diameter ~ 350nm) are highlighted by arrows. **(B)** The ALP-expressing PHY2433 strain (TN124; Noda et al., 1995) was induced (−Dox), or not (+Dox; 10μg/ml), for Kes1 or kes1^{Y97F} expression. Cultures were maintained at an OD_{600nm} < 0.2 throughout, harvested and assayed for ALP activity. Error bars represent standard deviation. **(C)** PCA scores plot distinguishing the ^{1}H-NMR metabolic profiles of WT yeast (CTY182) expressing Kes1 or kes1^{Y97F} (− Dox), or not (+Dox). **(D)** Targeted PCA of individual metabolites was performed for each condition. Reductions in Arg, Asn, Asp, Glu, Gln, Thr, and Trp pools were the major contribution to the variance between conditions of excess Kes1/kes1^{Y97F} and mock controls. **(E)** WT yeast (CTY182) transformed with YCp(*URA3*), YCp(P_{DOX}*::KES1*) or YCp(P_{DOX}*::kes1*^{Y97F}) were spotted in 10-fold dilution series on media with Dox (10μg/ml) and amino acids (NEQR, 0.2% w/v). **(F)** *atg13Δ* yeast co-transformed with YEp(P_{CUP1}*::HA-ATG13*) and either YCp(P_{DOX}*::KES1*) or YCp(P_{DOX}*::kes1*^{Y97F}) were

cultured in media containing 10μg/ml Dox. *KES1* or *kes1*^{Y97F} expression was induced for 7 hours (−Dox), or not (+Dox; 10μg/ml), and cells were challenged with $CuSO_4$ (100μM for 1hr) to induce HA-Atg13 expression. HA-Atg13 species were visualized by immunoblotting with anti-HA antibodies. Also see Suppl. Figs. S3, S4 and S5.

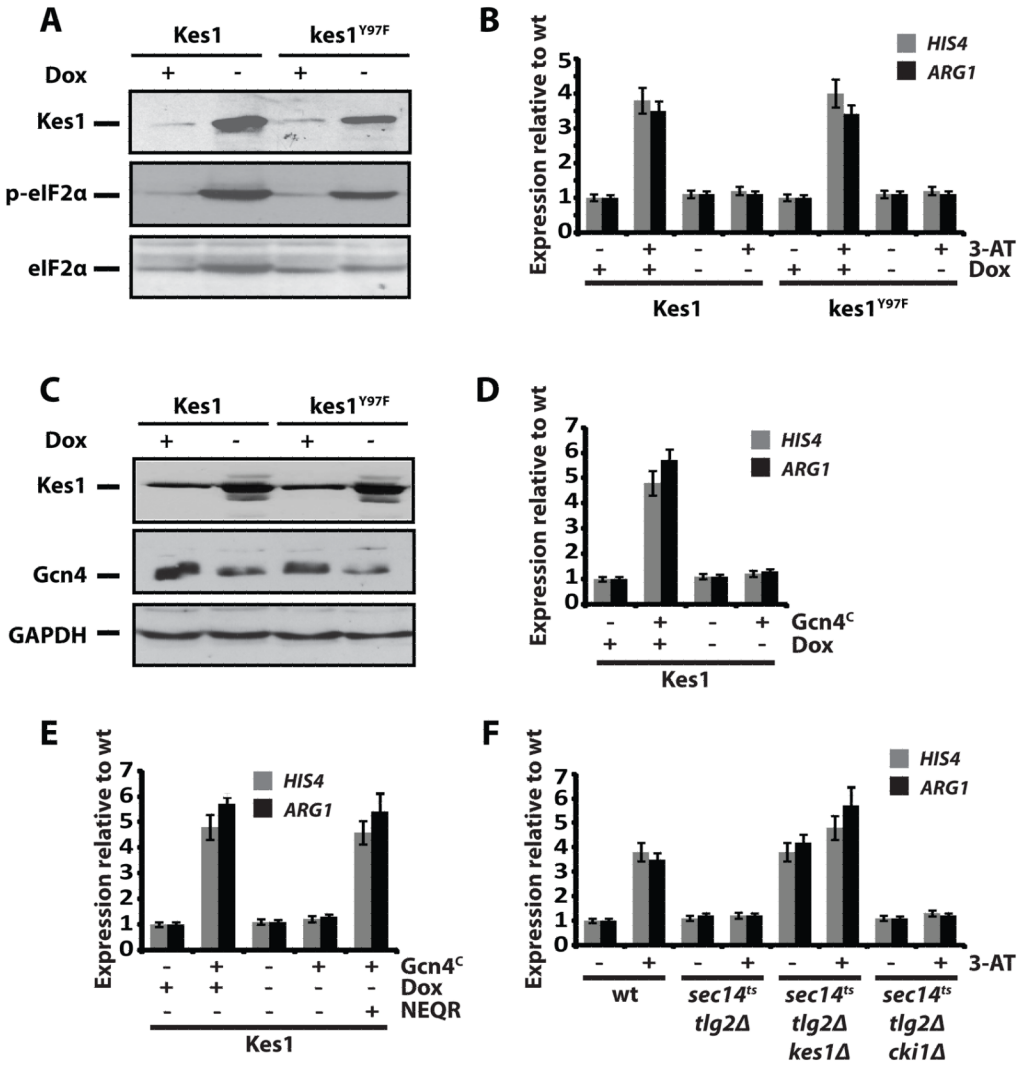

Figure 4.

Kes1 attenuates Gcn4-dependent activation of the general amino acid control. **(A)** Lysates were prepared from paired cell cultures induced for Kes1 or kes1^{Y97F} expression (−Dox), or not (+Dox; 10μg/ml). Phospho-eIF2α, Kes1 and eIF2α were visualized by immunoblotting. **(B)** Total RNA was prepared from cells (CTY8-11Cα) induced for Kes1 or kes1^{Y97F} expression (−Dox), or not (+Dox) and challenged with 100mM 3-AT for 2 hours to induce the GAAC. *HIS4*, *ARG1* and *ACT1* expression was surveyed by RT-PCR. Error bars represent standard deviation. **(C)** Gcn4, Kes1 and GAPDH were analyzed by immunoblotting of lysates prepared from WT cells (CTY8-11Cα) expressing Kes1 or kes1^{Y97F} (−Dox) or not (+Dox). Cells were challenged with 100mM 3-AT for 2 hours to induce the GAAC. **(D)** Total RNA fractions were isolated from WT cells harboring YCp(P_{DOX}*::KES1*) and co-transformed with YCp (*TRP1*) or YCp (*GCN4^{C}*) cultured +/− Dox. *HIS4* and *ARG1* gene expression was surveyed by RT-PCR, and normalized to *ACT1* expression. Undiluted product and a 4-fold dilution of product was analyzed. Error bars represent standard deviation. **(E)** The experiment is as in (D) with the modification that an NEQR cocktail (0.2% w/v) was added to a parallel culture induced for Kes1 expression. *HIS4*, *ARG1* and *ACT1* expression were scored by RT-PCR. Error bars represent standard deviation. **(F)** RT-PCR of GAAC target genes *ARG1* and *HIS4*, as well as *ACT1* control

from total RNA fractions prepared from WT, *sec14-1^{ts} tlg2Δ*, *sec14-1^{ts} tlg2Δ kes1Δ* or *sec14-1^{ts} tlg2Δ cki1Δ* cells shifted to 37°C for 2hrs to impose the strong *sec14-1^{ts} tlg2Δ*-associated TGN/endosomal trafficking block. Error bars represent standard deviation. Also see Suppl. Fig. S6.

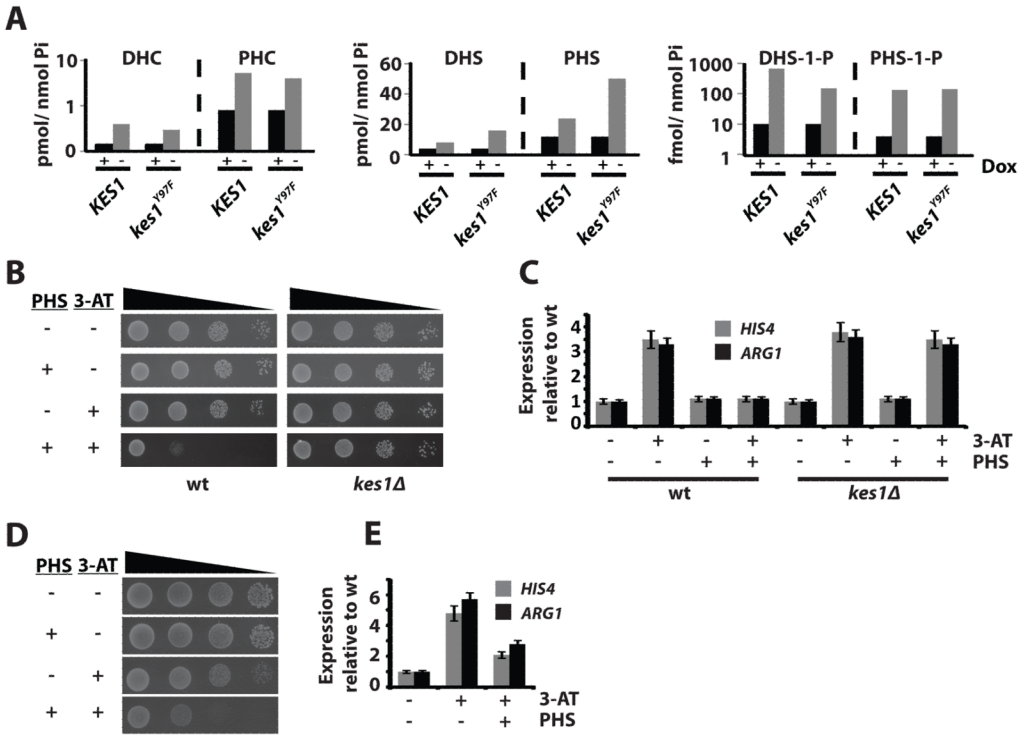

Figure 5.

Sphingolipids inhibit the GAAC. **(A)** Quantitative lipidomics of DHC, PHC, DHS, PHS, DHS-1-P and PHS-1-P in yeast (CTY182) as a function of Kes1 or Kes1^{Y97F} expression. Note the $\log_{10}$ scale for the *y*-axis. **(B)** WT strain (CTY8-11Cα) and a *kes1Δ* derivative were spotted in a 10-fold dilution series on synthetic complete (SC) media and SC media with 7.5μM PHS, with 10mM 3-AT, or both. **(C)** Total RNA fractions were isolated from WT yeast either mock treated or grown in the presence of 7.5μM PHS for 2 hours. Cells were either mock-treated or challenged with 100mM 3-AT for 2 hours to induce the GAAC. *HIS4*, *ARG1* and *ACT1* expression were monitored by RT-PCR. Undiluted product and a 4-fold dilution of product were analyzed. Error bars represent standard deviation. **(D)** WT yeast (CTY8-11Cα) expressing Ura3 or Gcn4^{c} were spotted in a 10- fold dilution series on SC media and SC media with 7.5μM PHS, with 10mM 3-AT, or both. **(E)** Total RNA fractions were prepared from WT yeast expressing Ura3 or Gcn4^{c} +/− 15μM PHS for 2 hrs. *HIS4* and *ARG1* expression was surveyed by RT-PCR and normalized to *ACT1* expression. Undiluted product and a 4-fold dilution of product were analyzed. Error bars represent standard deviation. Also see Suppl. Fig. S7.

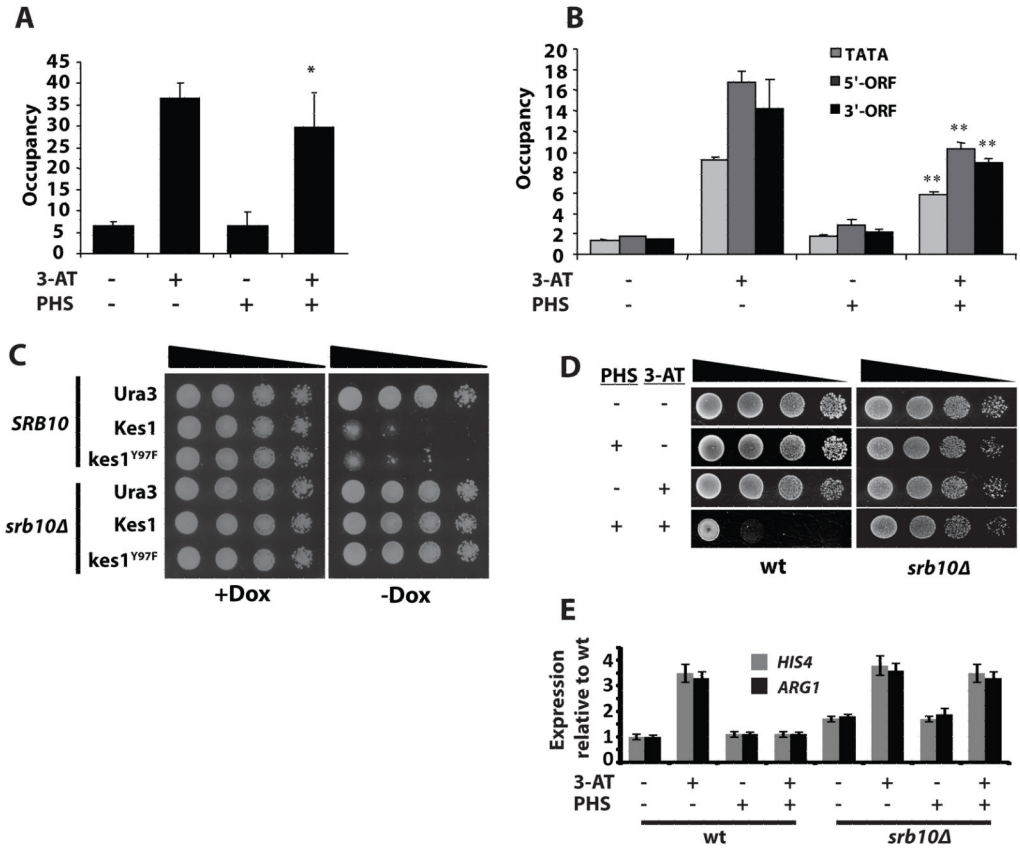

Figure 6.

Gcn4 binding to target genes and Mediator. **(A)** Cells were treated with PHS (15μM) for 2 hrs prior challenge with 3-AT (10mM) for 30 min, and perfused with formaldehyde. Sonicated chromatin was precipitated with antibodies against Gcn4 (A) or Rpb3 (B). DNA extracted from immunoprecipitates (ChIP) or starting chromatin (input) was PCR-amplified in the presence of [^{32}P]-dATP with primers for *ARG1* UAS (A), TATA element, or sequences from the 5′ or 3′ end of the *ARG1* coding sequences (B), and with primers for an intergenic chromosome V sequence (nonspecific control). PCR products were quantified by phosphorimaging. Ratios of *ARG1* ChIP-to-input signals were normalized against chromosome V control sequence ratios to yield occupancy values. Averages and standard errors from 2 PCR amplifications for each of 2 independent immunoprecipitates from 2 independent cultures are plotted. Error bars represent standard deviation. **(C)** Isogenic WT (CTY1740) and *srb10Δ* yeast harboring YCp vectors for Dox-repressible expression of Kes1 were spotted in 10-fold dilutions series on media +/− Dox (10μg/ml) and incubated at 30°C. **(D)** Isogenic WT (CTY1740) and *srb10Δ* yeast were spotted in a 10-fold dilution series on media with 7.5μM PHS, with 10mM 3-AT, or both 7.5μM PHS and 10mM 3-AT. **(E)** Isogenic WT (CTY1740) or *srb10Δ* yeast were either mock treated, or challenged with 15μM PHS for 2 hrs. The cultures were challenged with 100mM 3-AT for 2 hrs to induce the GAAC. *HIS4*, *ARG1* and *ACT1* expression was monitored by RT-PCR. Undiluted product and a 4-fold dilution of product was analyzed. Error bars represent standard deviation.

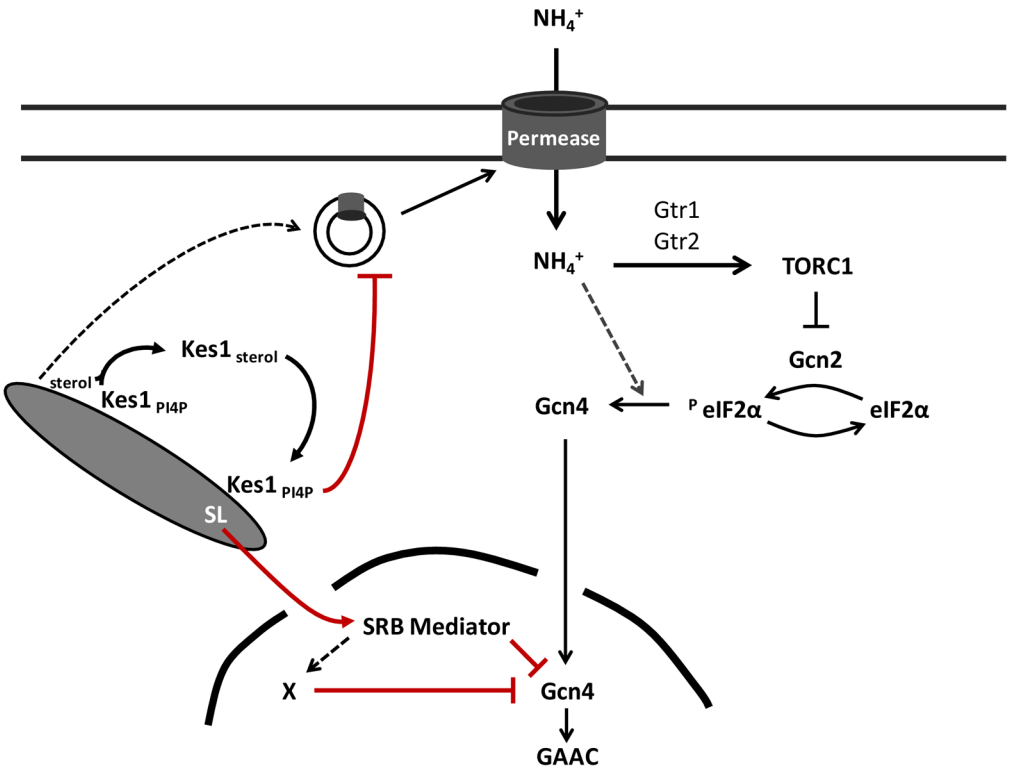

Figure 7.

Integration of TGN/endosomal trafficking flux to transcriptional competence of the nitrogen response. **(A)** Membrane trafficking through a signaling TGN/endosomal compartment is defined by Sec14-regulated production of PtdIns-4-P countered by Kes1-mediated PtdIns-4-P sequestration. Degree of sequestration is set by PtdIns-4-P-mediated recruitment of Kes1 to TGN/endosomal membranes, and released by binding of the membrane-bound Kes1 to active sterol. **(B)** Kes1-mediated trafficking defects reduce efficiency of amino acid and NH_4^+ permease delivery to the plasma membrane. The incipient nitrogen stress results in reduced TOR activity and engagement of the early stages of the GAAC (phosphorylation of eIF2α). Efficiency of the terminal stages of the GAAC is determined by potency of Gcn4 antagonism levied by activity of the large SRB Mediator complex. **(C)** Potency of a Kes1-mediated trafficking arrest/delay sets the amplitude of TGN/endosomal production of SL available for nuclear signaling. SL* denotes a sphingolipid with signaling power (e.g. ceramide) produced in TGN/endosomal compartments. The potency of SL* signaling is directly proportional to Kes1 activity, and inhibits transcription initiation/elongation of genes loaded with Gcn4 and RNA polymerase II via action of the CDK8 module of the large SRB Mediator complex. SL* signaling foils the GAAC and induces cells to enter a metabolically coherent quiescence with properties of post-mitotic cell physiology.